coatings

MDPI

Article

PH-Responsive Sodium Alginate Edible Films Incorporated with Grape Seed Proanthocyanidins and Thyme Essential Oil for Pork Preservation

Guoyou Yin [1], Yulin Liu [1], Jie Sun [1,*], Xin Wang [1], Yakun Li [2], Yuqi Cao [1], Zhuofan Yang [1], Luyang Wang [1] and Peipei Li [2]

[1] College of Life Science and Engineering, Henan University of Urban Construction, Pingdingshan 467036, China
[2] Henan Fengrui Food Co., Ltd., Pingdingshan 467300, China
* Correspondence: 30110503@huuc.edu.cn

Abstract

To meet the demand for edible packaging materials that possess both pH-responsive properties and antibacterial performance in the field of meat preservation, this study developed an edible GSP-TEO-SA film using sodium alginate (SA) as the film-forming substrate, thyme essential oil (TEO) as the antibacterial agent, and grape seed proanthocyanidins (GSP) as the pH-responsive component. The effects of GSP and TEO addition on the structure, mechanical properties, antioxidant activity, and antibacterial activity of the edible film were systematically evaluated, and its practical application effectiveness in pork preservation was investigated. The results indicated that the addition of 0.5% GSP significantly enhanced the tensile strength, UV barrier properties, and antioxidant efficacy of the edible film ($p < 0.05$). The incorporation of 1% TEO increased the hydrophobicity of the film. When GSP and TEO were present simultaneously, the tensile strength and elongation at break of the film increased to their maximum values, reaching 3.81 ± 0.04 MPa and 57.76 ± 1.97%, respectively. Furthermore, the film exhibited the lowest water vapor transmission rate and the largest contact angle of 65.70°. Fourier transform infrared spectroscopy and thermogravimetric analysis revealed altered or strengthened hydrogen-bonding interactions within the GSP-TEO-SA film, leading to a denser and more stable structure. In pork preservation applications, both the GSP-SA film and the GSP-TEO-SA film exhibited color changes, with the most pronounced alteration observed in the GSP-TEO-SA film. Meanwhile, during storage, the GSP-TEO-SA film effectively inhibited the increases in pH, TVB-N content, and total viable count. In conclusion, the GSP-TEO-SA film holds great promise for meat preservation applications.

Keywords: edible film; intelligent packaging; antibacterial activity; freshness monitoring

Check for updates

Academic Editor: Rafael José Gavara

Received: 22 September 2026
Revised: 24 October 2026
Accepted: 30 October 2026
Published: 1 November 2026

Copyright: © 2026 by the authors. Licensee MDPI, Basel, Switzerland. This article is an open access article distributed under the terms and conditions of the Creative Commons Attribution (CC BY) license.

1. Introduction

Food packaging serves as a crucial tool for food preservation, transportation, storage, and marketing [1]. Traditional food packaging typically utilizes petroleum-based polymers as the primary packaging materials, providing a physical barrier that protects food from adverse environmental factors such as microbial contamination, physicochemical damage, and light exposure, thereby extending the shelf life of food products [2]. However, traditional packaging exhibits poor biodegradability and is prone to causing environmental issues such as plastic pollution. Moreover, it fails to promptly detect or respond to quality deterioration

within the package or changes in the storage environment, which can easily lead to food waste and even potential food safety incidents [3]. Therefore, to meet the demand for rapid, accurate, and visual freshness detection, researchers have begun extensively studying intelligent color-changing freshness detection methods. Among these, pH-responsive food composite films, as a form of intelligent packaging, have emerged as a prominent research focus among scholars globally in recent years [4].

pH-responsive composite films can accurately respond to changes in the acidity/alkalinity of food packaging environments, exhibiting distinct color changes to monitor food quality in real time [5,6]. However, selecting suitable matrix materials and indicators remains a critical challenge in enhancing film performance. Sodium alginate (SA), a natural plant polysaccharide, is widely used as a film-forming matrix due to its excellent film-forming properties. The carboxyl groups in its molecular structure can form hydrogen bonds with polyphenolic substances, providing a structural basis for pH-responsive functionality. However, pure sodium alginate films suffer from drawbacks such as poor mechanical properties, high brittleness, and low barrier performance, which limit their application in food packaging [7]. The incorporation of plant essential oils not only enhances the mechanical and barrier properties of the edible film, but when combined with sodium alginate, they also exhibit a synergistic effect in improving the film's antioxidant and antibacterial performance [8]. Thyme essential oil (TEO) mainly contains thymol and carvacrol. These compounds can disrupt the integrity of bacterial cell membranes, leading to the leakage of intracellular contents and thereby exerting antibacterial activity. In addition, their phenolic hydroxyl groups can scavenge free radicals, thus conferring antioxidant activity [9]. Researchers have incorporated thyme essential oil into edible films to enhance their antimicrobial and water barrier properties. Guzmán-Pincheira et al. evaluated composite films of alginate and chitosan incorporated with thyme essential oil, reporting improvements in both the mechanical properties and antimicrobial capacity of the films [10]. Liu et al. incorporated thyme essential oil into konjac glucomannan-based films and found that it significantly improved the physical properties of film while enhancing its antioxidant and antimicrobial activity [11]. Anthocyanins are water-soluble flavonoid pigments with antioxidant and antibacterial activities, and have been widely used as indicators in intelligent packaging systems [12,13]. However, anthocyanins exhibit poor thermal stability (easily degraded above 60 °C) and insufficient compatibility with antibacterial components, which can easily lead to structural defects in the film. The discovery of grape seed proanthocyanidins (GSP) offers a new perspective for overcoming the aforementioned limitations. Grape seed proanthocyanidins (GSP) are a class of natural polyphenols, polymerized from catechin and epicatechin as monomeric units. They are rich in phenolic hydroxyl groups and can efficiently scavenge free radicals and chelate metal ions, thereby exhibiting strong antioxidant capacity. As such, GSP is a natural antioxidant widely used in active food packaging. To date, GSP or TEO have each been individually incorporated into polysaccharide-based film-forming systems to achieve pH-responsive function or antimicrobial preservation effects, respectively [10,11,14]. However, studies that combine GSP with TEO to simultaneously construct composite films with both pH color-responsive and antimicrobial multifunctionality, and to evaluate their practical performance in chilled pork preservation, remain limited.

Therefore, this study utilizes SA as the film-forming matrix, TEO as the antibacterial agent, and GSP as the pH-responsive component to develop a novel edible food film. The structure, mechanical properties, antioxidant activity, and antibacterial activity of the film will be systematically investigated. Additionally, the film's antibacterial efficacy and color-indicating function in pork preservation will be evaluated. This work aims to provide a

theoretical foundation for the development and application of multifunctional edible food packaging films.

2. Materials and Methods

2.1. Materials

SA were provided by Henan Qihuali Biotechnology Co., Ltd (Zhengzhou, China). The thyme essential oil used in this study (purity approximately 99%) was purchased from Lvzhang Biotechnology Co., Ltd (Guangzhou, China). The composition was provided by the manufacturer, and its main components of the thyme essential oil are as follows: The main components of the thyme essential oil are as follows: carvacrol (43.23%), thymol (35.46%), and p-cymene-2,5-diol (10.05%). The grape seed proanthocyanidins (GSP) used in this study (purity approximately 98%) were provided by Huajian Biotechnology Co., Ltd. (Zhuhai, China). The composition of GSP is as follows: flavan-3-ol monomers (14.6%), dimers (23.4%), trimers (6.8%), and proanthocyanidin oligomers (5–13 structural units; 52.4%). Pork tenderloin was obtained from Pingdingshan Dexinquan Supermarket (Pingdingshan, China). Glycerin was purchased from Beijing Solaibao Technology Co., Ltd (Beijing, China). 2,2-diphenyl-1-picrylhydrazy (DPPH), 2,2-azinobis-(3-ethylbenzothiazoline-6-sulfonic acid) (ABTS) were purchased from Shanghai Yuanye Biotechnology Co., Ltd (Shanghai, China). *Escherichia coli* (ATCC25922) and *Staphyloccocus aureus* (ATCC29213) were stored at the Laboratory of Food Processing and Components, Henan University of Urban Construction. All other reagents were of analytical grade.

2.2. Preparation of Composite Films

Four grams of sodium alginate were dissolved in 400 mL of distilled water, and 6 g of glycerol was added, followed by 5 min of stirring. The mixture was then divided into four equal portions, each serving as one of the four experimental groups. One group was left untreated and labeled as SA. To the second group, 0.5 g of grape seed proanthocyanidins (GSP) (0.5% w/v) was added, labeled as GSP-SA. The third group received 1 g of thyme essential oil (TEO) (1% w/v) and was labeled as TEO-SA. The final group received both 1 g of thyme essential oil and 0.5 g of grape seed proanthocyanidins, labeled as GSP-TEO-SA (Table 1). Each mixture was stirred until uniformly dispersed, then left to stand for 12 h for deaeration. The film-forming solutions were subsequently poured into Petri dishes and dried at 40 °C. Finally, the dried films were immersed in a 10% glycerol solution for 20 s as a post-plasticization treatment to improve the flexibility of the films, equilibrated at room temperature for 12 h, and then peeled off and used for subsequent experiments.

Table 1. Formulations of the edible films.

Edible Film	GSP/(g)	TEO/(g)	Distilled Water/mL	SA/(g)	Glycerol/(g)	Mass Concentration (w/v)
SA	0	0	100	1	1.5	0
GSP-SA	0.5	0	100	1	1.5	0.5
TEO-SA	0	1	100	1	1.5	1.0
GSP-TEO-SA	0.5	1	100	1	1.5	1.5

2.3. Characterization

2.3.1. Thickness and Mechanical Property

The film thickness was measured with a micrometer by selecting three samples per group and measuring one central and two peripheral random points on each. The average was calculated and recorded as the sample thickness.

The tensile strength (TS) and elongation at break (EB) of films were determined with a texture analyzer (TMS-PRO, Food Technology Corporation, Sterling, Virginia, USA) using strips (10 mm × 70 mm) at a speed of 0.5 mm/s, according to Equations (1) and (2).

$$TS(MPa) = \frac{F}{TW} \quad (1)$$

$$EB(\%) = \frac{L - L_0}{L_0} \times 100\% \quad (2)$$

where F is the maximum force at fracture (N), T is the film thickness (m), W is the film width (m), L is the extended length at fracture (m), and L_0 is the original length (m).

2.3.2. Color Characterization of Films

Color of the films at pH 7 was measured using a colorimeter (WSC-S, Shanghai Yidian Physical Optical Instrument Co., Ltd., Shanghai, China). A standard white plate was used as a reference to determine the L* (lightness), a* (green to red), and b* (blue to yellow) values of the films. The total color difference (ΔE) was calculated according to Equation (3).

$$\Delta E = \sqrt{\Delta a^2 + \Delta b^2 + \Delta L^2} \quad (3)$$

where $\Delta a = a^*_{standard} - a^*_{sample}$; $\Delta b = b^*_{standard} - b^*_{sample}$; $\Delta L = L^*_{standard} - L^*_{sample.}$ The L*, a*, and b* values of the standard whiteboard were measured as follows: L* standard = 98.25; a*standard = 1.12; b*standard = −1.588.

2.3.3. Measurement of Opacity and Transmittance

The opacity and transmittance of films were determined based on the method described by Wu et al. with modifications [15]. Rectangular film samples (30 mm × 10 mm) were prepared, and their absorbance at wavelengths of 600 nm and 400 nm was measured using a UV-visible spectrophotometer (T60, UV/Vis spectrometer, PG Instruments Ltd., Wibtoft, UK). The opacity and light transmittance were then calculated according to Equations (4) and (5), respectively.

$$Opacity(A \cdot mm^{-1}) = \frac{A_{600}}{d} \quad (4)$$

Here, A_{600} represents the absorbance at 600 nm, and d represents the thickness of the films (mm).

The transmittance (T%) of the film was calculated using the following formula:

$$T(\%) = 0.1^A \times 100\% \quad (5)$$

Here, A is the absorbance of films at 400 nm, and T is the transmittance of films.

2.3.4. Determination of Water Vapour Transmission Rate (WVTR) and Contact Angle

The barrier property of the film was evaluated by measuring its water vapour transmission rate, following the method described by Tan et al. [16]. Specifically, 2 g of silica gel was weighed and placed into a centrifuge tube, the opening of which was sealed with the film sample. The tube was then weighed and kept at 25 °C for 24 h (with the relative humidity on the silica gel side maintained at 0% RH) before being weighed again. This process was repeated three times, and the average value of the three weight measurements was taken. WVTR was calculated according to Equation (6).

$$WVTR(g/(m^2 \cdot 24\ h)) = \frac{24 \cdot \Delta m}{t \cdot A} \quad (6)$$

where t represents time (h), A represents the cross-sectional area of the centrifuge tube opening (m^2), and Δm represents the change in weight of the glass bottle (g).

The surface hydrophobicity of the edible film was evaluated by measuring the water contact angle (θ) with a video optical contact angle meter (JC2000D, Shanghai Kuncheng Scientific Instrument Co., Ltd., Shanghai, China) by placing a drop of ultrapure water (10 μL) on the surface of the films according to the method described by Zhao et al. [17].

2.3.5. Structure and Morphology Characterization

The surface and cross-sectional morphologies of the films were examined by scanning electron microscopy (Hitachi SU8600, Hitachi High-Tech Corporation, Tokyo, Japan) after freeze-fracturing in liquid nitrogen, gold sputter-coating, and scanning at 1.5 kV. Infrared spectroscopy (PerkinElmer Spectrum, Perkinelmer Enterprise Management (Shanghai) Co., Ltd., Shanghai, China) was used to determine the chemical structure and potential interactions of composite films and the scanning range was 4000 cm^{-1} to 650 cm^{-1} with a resolution of 4 cm^{-1}. The crystal structure of the films was investigated using an X-ray diffractometer (XRD, Ultima IV, Rigaku Corporation, Tokyo, Japan) with Cu-Kα radiation (λ = 1.542 Å) at 40 kV and 100 mA, using a scan rate of 4 °/min and a step size of 0.02° over a 2θ range of 5° to 60°. The thermal stability of the composite film was determined according to the method of Sun et al. [18]. Film samples were cut into small pieces, and 10 mg of each was weighed and heated from 30 °C to 600 °C at a rate of 10 °C/min under a constant nitrogen flow (20 mL/min) for analysis.

2.3.6. Functional Properties of Edible Films

Antioxidant activities: Following the methodology proposed by Sun et al., the antioxidant activity of the edible films can be evaluated by measuring the DPPH scavenging rate and ABTS radical scavenging rates [19]. 0.5 g of film was cut into small pieces and immersed in 10 mL of deionized water. Then, 50 μL of the sample solution was mixed with 120 μL of DPPH ethanol solution (0.2 mmol/L). The mixture was kept in the dark at room temperature for 30 min, and the absorbance was measured at 517 nm using a UV-Vis spectrophotometer. The scavenging rate was calculated as:

$$\text{DPPH radical scavening rate}(\%) = \frac{A_0 - A_1}{A_0} \times 100\% \quad (7)$$

where A_0 is the absorbance of the blank control DPPH at 517 nm, and A_1 is the absorbance of the sample at 517 nm.

For the ABTS assay, the ABTS radical working solution was prepared by mixing ABTS stock solution with potassium persulfate and allowing the reaction for 12–16 h in the dark. The absorbance was adjusted to 0.70 ± 0.02 at 734 nm. Then, 30 μL of sample solution was mixed with170 μL of ABTS working solution, and the absorbance was measured at 734 nm. The scavenging rate was calculated as:

$$\text{ABTS radical scavening rate}(\%) = \frac{A_0 - A_1}{A_0} \times 100\% \quad (8)$$

where A_0 is the absorbance of the blank control ABTS at 734 nm, and A_1 is the absorbance of the sample at 734 nm.

Antibacterial activity: The antibacterial activity of the composite film against *Escherichia coli* (*E.coli*) and *Staphylococcus aureus* (*S.aureus*) was evaluated using a liquid culture method [20]. A 0.2 g film sample was immersed in a culture medium containing 10^5 CFU/mL of bacterial inoculum, and a bacterial suspension without film was used as the control. After incubation at 37 °C for 24 h and 48 h intervals, 1 mL aliquots were collected, and the optical density at 600 nm was measured with a spectrophotometer (T60, UV/Vis spectrometer, PG Instruments Ltd., Wibtoft, UK). The antibacterial activity was determined by assessing the inhibition of bacterial growth based on changes in the turbidity of the bacterial suspension.

2.3.7. Analysis of pH-Sensitive Properties

0.5 g of GSP was dissolved in 7 mL of 0.1 M PBS at varying pH levels (4–12) for 2 min, and the resulting solution colors were observed. GSP-SA and GSP-TEO-SA film-forming solutions were prepared. Their pH was adjusted to 4–12 using diluted 0.1M HCl and 0.2 M NaOH, the pH was measured using a Lei-ci (Shanghai INESA Scientific Instrument Co., Ltd., Shanghai, China) PHS-3E pH meter, and color changes were recorded. Simultaneously, the films cast from these solutions at different pH values were observed for color variation until the color no longer changed.

2.3.8. Preservation Effect of Edible Films on Pork

Edible films with uniform size and shape were selected for preservation experiments. Fresh pork loin slices (10 g each) were equally divided, wrapped with different films, and stored in a refrigerator at 4 °C. Unwrapped slices served as the control group. On days 0, 2, 5, 7, and 10 of storage, the wrapped pork slices were homogenized with 100 mL of saline, followed by gradient dilution. An appropriate dilution of the homogenate was spread on agar plates, cultured, and counted, with results expressed as lg CFU/g. Additionally, color changes in the GSP-SA and GSP-TEO-SA films were observed on days 0, 2, 5, 7, and 10. On days 0, 2, 5, 7, and 10, 5 g of pork sample was homogenized with 45 mL of distilled water, and the pH value was measured using a calibrated pH meter. TVB-N was determined according to the Chinese national standard GB 5009.228-2016 using an automatic Kjeldahl nitrogen analyzer, and the results were expressed as mg/100 g. The spoilage threshold of TVB-N was set at 20 mg/100 g, and the pH spoilage threshold was 6.7 according to GB/T 5009.237-2016.

2.4. Statistical Analysis

All experiments were performed with three independent film preparations. Each sample was measured three times, and the average was used for statistical analysis. The results are expressed as mean ± standard deviation. Each film formulation was treated as an independent group, and pork samples at different storage time points were also analyzed as independent groups. Significant differences among groups were assessed by one-way analysis of variance (ANOVA), followed by Tukey's HSD post hoc test, with a significance level of $p < 0.05$. Statistical analysis was conducted using IMB SPSS 25 (IBM Inc., Armonk, NY, USA), and figures were plotted using Origin 2022 (Origin lab Software Corp, Northampton, MA, USA).

3. Results and Discussion

3.1. Thickness and Mechanical Properties Analysis

The thickness and mechanical properties of the films are shown in Figure 1. The thickness of all edible films ranged between 0.140 and 0.146 mm. The addition of GSP increased the film thickness in the two corresponding groups, possibly due to the increased content of dry matter within the film matrix [21]. In contrast, the incorporation of TEO did not cause a significant change in thickness, likely because its added amount was relatively low and thus exerted a minimal effect. TS and EB are related to the intermolecular binding forces and the hydrogen bonding capacity between hydroxyl groups [22]. GSP and TEO had distinct effects on EB of the films. Compared to the pure SA film, TS increased in all three modified groups. Specifically, TS of the GSP-SA film increased significantly by 28.20% ($p < 0.05$). The GSP-TEO-SA film exhibited the highest TS, with a significant increase from 2.85 ± 0.04 MPa to 3.81 ± 0.04 MPa ($p < 0.05$). The EB of the GSP-SA group decreased slightly compared to the SA group, from 38.38 ± 0.78% to 37.57 ± 2.02%, although the

difference was not statistically significant. This could be attributed to the formation of stronger hydrogen bonds between the added GSP and the SA chains, which enhanced the film's rigidity while reducing its extensibility [23]. Conversely, the films containing TEO showed an increase in EB, indicating improved flexibility and extensibility.

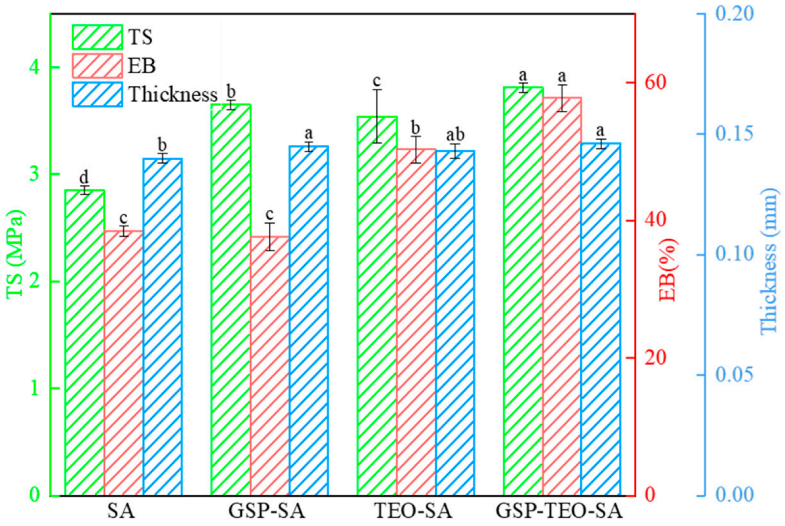


Figure 1. Thickness, tensile strength, and elongation at break of edible films. Note: Different letters indicate significant differences(a–d) ($p < 0.05$)

3.2. Color Measurement

Color parameters L, a, and b values of the edible films are shown in Table 2. The SA film without GSP exhibited the highest brightness. After the addition of GSP, the brightness of GSP-SA and GSP-TEO-SA films decreased by 25.42% and 29.31%, respectively, compared to the SA film. Meanwhile, due to the reddish-brown color of GSP, both a and b values increased significantly ($p < 0.05$), indicating that the films became redder and more yellowish [24]. The addition of TEO also slightly increased the a, b, and L* values of the TEO-SA film, but its ΔE relative to the white plate was smaller than that of the SA film relative to the white plate. The combined effect of GSP and TEO was the most pronounced, with the L value of the GSP-TEO-SA film decreasing by 34.33% compared to the SA film, while the a, b, and ΔE values increased significantly ($p < 0.05$).

Table 2. Color Changes in Edible Film.

Edible Films	L*	a*	b*	ΔE
SA	68.34 ± 0.20 ^{a}	1.13 ± 0.03 ^{c}	−1.51 ± 0.02 ^{c}	29.91 ± 0.20 ^{c}
GSP-SA	50.97 ± 0.23 ^{b}	21.00 ± 0.40 ^{b}	18.04 ± 0.09 ^{b}	54.92 ± 0.38 ^{b}
TEO-SA	67.97 ± 0.80 ^{a}	1.81 ± 0.10 ^{c}	−1.18 ± 0.05 ^{c}	30.28 ± 0.80 ^{c}
GSP-TEO-SA	48.31 ± 0.41 ^{c}	22.56 ± 0.28 ^{a}	20.50 ± 0.45 ^{a}	58.66 ± 0.49 ^{a}

Note: Different letters indicate significant differences(a–c) ($p < 0.05$).

3.3. Optical Properties of the Films

The light transmittance and opacity of the edible films are shown in Figure 2A. The inherent color of GSP contributes to its influence on film opacity. The monomers such as epicatechin gallate contained in GSP can enhance the compactness of the film structure. As a phenolic compound, GSP also effectively absorbs ultraviolet light [25]. Therefore, the light transmittance of the GSP-SA and GSP-TEO-SA films decreased significantly at 400 nm ($p < 0.05$), indicating improved UV-shielding at 400 nm, an effect that helps reduce damage

to food products. Moreover, the incorporation of GSP may promote the formation of cross-linked structures, and its combined effect with TEO further enhances the light-blocking properties of the films [26]. The UV transmittance of the GSP-TEO-SA film was only 17.65%. In addition, the opacity of the films at 400 nm increased markedly after the addition of GSP. The opacity values of the GSP-SA and GSP-TEO-SA films increased to 4.04 ± 0.01 and 4.21 ± 0.01 A·mm^{-1}, respectively, whereas that of the SA film was only 0.26 ± 0.02 A·mm^{-1}.

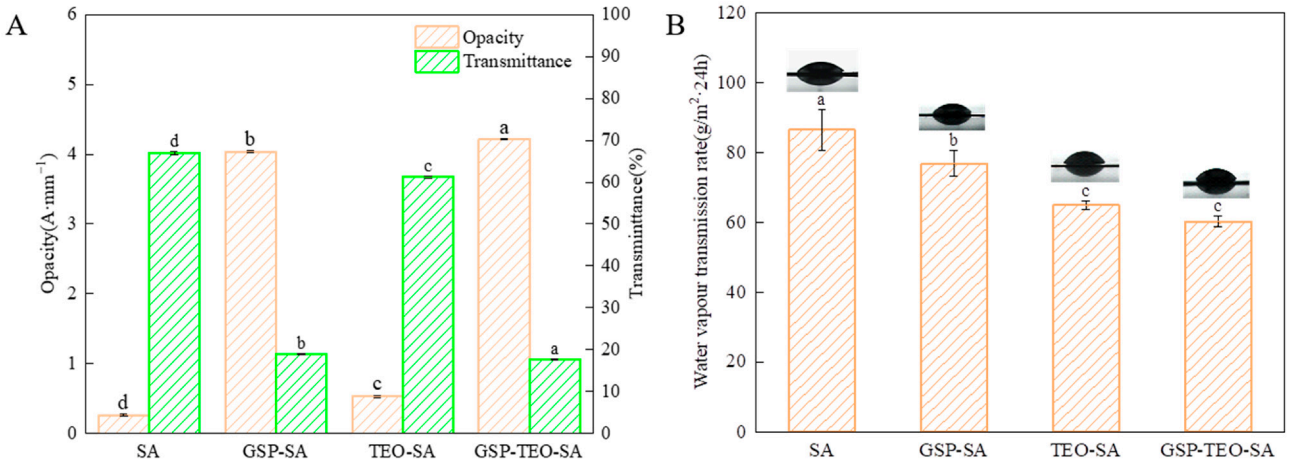


Figure 2. Light transmittance and opacity (**A**), water vapor transmission rate and contact angle (**B**) of edible films. Note: Different letters indicate significant differences (a–d) ($p < 0.05$).

3.4. Analysis of Water Vapour Transmission Rate (WVTR) and Contact Angle

Packaging with low water vapour transmission rate (WVTR) can delay food spoilage [27]. The WVTR of the edible films is shown in Figure 2B. The WVTR of the SA film was 85.35 ± 2.21 g/(m^2·24 h), while the other three composite films showed a decreasing trend. This is because anthocyanin-like substances can readily form new hydrogen bonds within the film matrix, disrupting its original spatial structure. This increases the internal free volume of the edible film, allowing water molecules to pass through more easily and consequently increasing the WVTR [28]. Although GSP is similar to anthocyanins in containing a large number of hydroxyl functional groups, its incorporation did not increase the WVTR, indicating a relatively intact internal film structure. Furthermore, the reduced WVTR observed in TEO-SA and GSP-TEO-SA is primarily related to the hydrophobic nature of TEO. During the drying process, TEO may have flocculated, forming oil droplets dispersed within the internal free volume of the film. This impedes the diffusion of water vapor, leading to the decrease in WVTR [29].

Contact angle is a common method for determining the hydrophobicity of edible films. A contact angle greater than 90° indicates a hydrophobic surface [30]. As shown in Figure 2B, the contact angles of all four films were below 90°, indicating their hydrophilic nature. The GSP-TEO-SA film exhibited the largest contact angle, 65.70 ± 0.94°, suggesting it possessed the highest hydrophobicity among them. The SA and GSP-SA films showed smaller contact angles, corresponding to poorer hydrophobicity. The significant increase in contact angles for the TEO-SA and GSP-TEO-SA films demonstrates the important influence of essential oil incorporation on the film's contact angle [31]. Concurrently, the decrease in WVTR observed in the previous results also supports that this change is likely attributable to the addition of TEO. However, the contact angle of the TEO-SA film 63.68 ± 0.82° remained below 90°. This could be due to the relatively low amount of TEO added and the fact that the film matrix is primarily composed of hydrophilic sodium alginate [32].

3.5. Structure Analysis

The surface and cross-sectional structures of films were observed by SEM, and the results are shown in Figure 3A. The surface of the SA film is relatively smooth but exhibits some cracks. The GSP-SA film displays a smooth surface with a continuous structure, and its cross-section is uniformly dense and crack-free. In contrast, both the TEO-SA film and the GSP-TEO-SA film incorporated with TEO show rougher and more irregular surfaces, along with the presence of bubbles. Their cross-sections reveal noticeable micropores or cavities, which are associated with the embedding of TEO droplets in the film matrix. During the film-forming process, TEO disperses uniformly in the film matrix initially, but droplet aggregation and flocculation may occur during drying, resulting in surface roughness and irregular cross-sectional morphology, consistent with findings reported in previous studies [33].

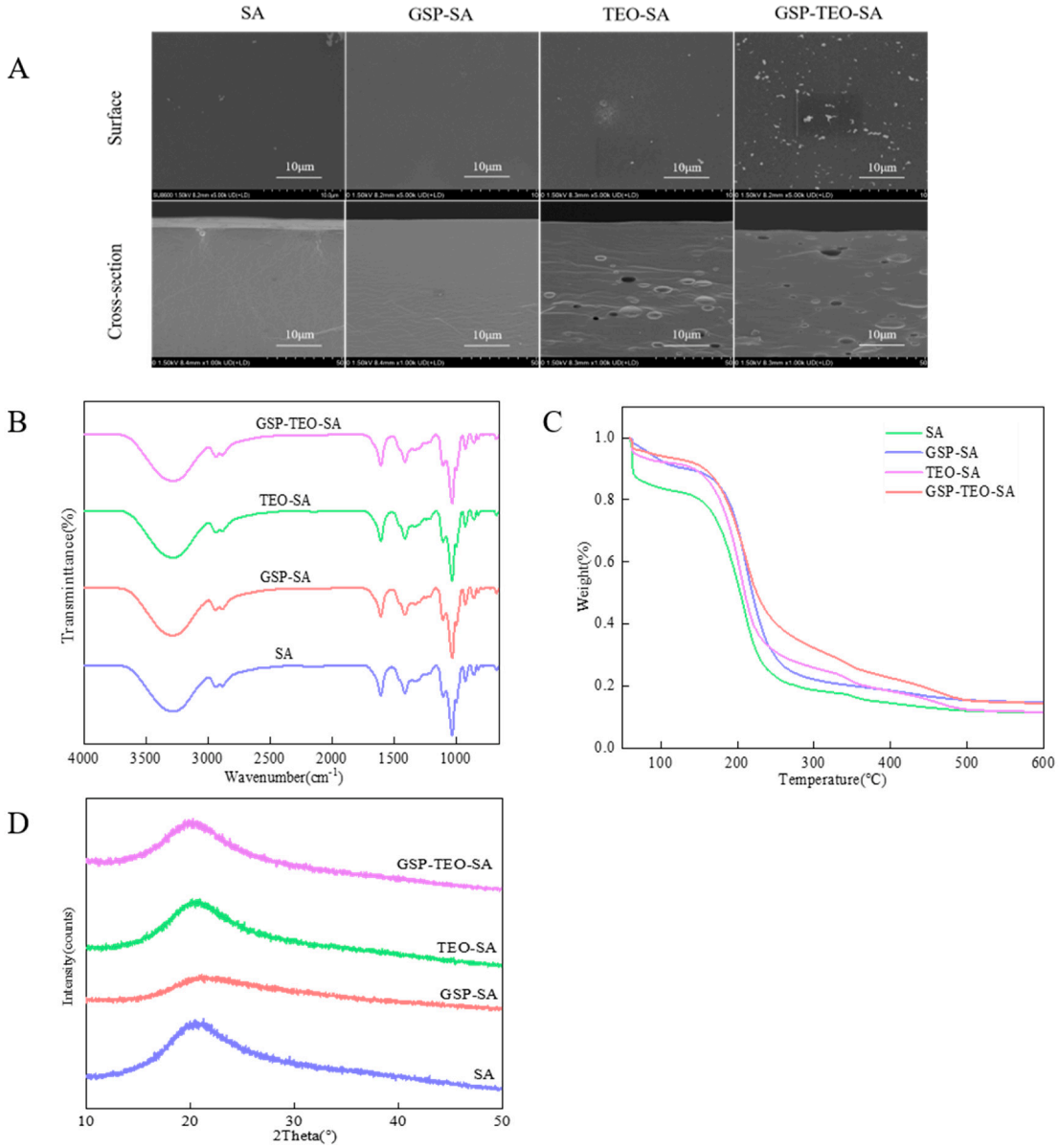


Figure 3. SEM images of the surface and cross-section (**A**), FTIR spectra (**B**), TGA curves (**C**), and XRD patterns (**D**) of edible films.

Fourier transform infrared spectroscopy (FTIR) was used to analyze the interactions between components in the edible films [34]. As shown in Figure 3B, the spectral profiles of

all films were similar, with the main peak corresponding to -OH/N-H stretching vibrations observed at 3275–3300 cm^{-1}. Upon the addition of GSP or TEO, this peak exhibited a red shift to the range of 3275–3285 cm^{-1}. The shift was most pronounced in the GSP-TEO-SA film, indicating altered or strengthened hydrogen-bonding interactions, which enhanced the structural stability of the film. The absorption peaks at 2933 cm^{-1} and 2882 cm^{-1} were attributed to the symmetric and asymmetric stretching vibrations of C-H bonds, while the peak in the range of 1600–1610 cm^{-1} corresponded to the vibrations of the carboxyl groups in SA [35]. Additionally, the sharp peak near 1030 cm^{-1}, associated with the asymmetric stretching of C-O-C bonds, displayed a blue shift in the GSP-SA, TEO-SA, and GSP-TEO-SA films compared to the SA film. This suggests that GSP and TEO influenced the polysaccharide structure [36].

Figure 3C shows the thermal stability of the edible films. The thermal decomposition process can be divided into three stages. The first stage (50–170 °C) is primarily attributed to the evaporation of adsorbed and bound water from the films, accompanied by the disruption of intermolecular hydrogen bonds. The extent of weight loss in this stage is related to the number of hydrogen bonds present [19]. The second stage (170–500 °C) corresponds to the decomposition of glycerol, SA, GSP, and TEO [37]. Films containing both GSP and TEO exhibit higher thermal stability. Notably, above 380 °C, the weight loss temperature of TEO is higher than that of GSP. In the third stage (500–600 °C), the film components undergo carbonization. The GSP-SA and GSP-TEO-SA groups show similar residual dry mass, which is greater than that of the other groups. This indicates that the addition of GSP increases the dry matter content of the films, while TEO does not significantly affect this property.

Figure 3D displays the XRD diffraction patterns of the different films. The pure SA film shows a strong characteristic diffraction peak at $2\theta = 21.04°$, indicating a well-defined crystalline structure. After the addition of TEO, the peak intensity decreases, suggesting a reduction in crystallinity. This may be due to hydrogen bonding between the hydroxyl groups of TEO and the carboxyl groups of SA, which disrupts the original crystalline network [38]. In the GSP-SA film, the overall diffraction peak intensity increases and the peak broadens. This could be attributed to the formation of a hydrogen-bonded network between the carboxyl groups of SA and the phenolic hydroxyl groups of GSP, introducing weakly crystalline domains and altering the crystalline state of the SA matrix [39]. In the GSP-TEO-SA composite film, the diffraction peak intensity further decreases compared to the TEO-SA and GSP-SA films, and the peak shape becomes sharper and narrower, with no other distinct diffraction peaks observed. This indicates that the addition of GSP contributes to enhanced crystallinity and suggests interactions among SA, TEO, and GSP [40].

3.6. Functional Analysis of Edible Films

The visual color changes in DPPH and ABTS radical solutions are shown in Figure 4A,B. The pure DPPH and ABTS radical solutions exhibited deep purple and deep blue-green colors, respectively. These assays were performed to characterize the intrinsic antioxidant activity of the edible films themselves. After treatment with the SA film, the solution colors showed no obvious change, indicating the weakest radical-scavenging ability of the SA film. In contrast, the TEO-SA group exhibited slight fading, which was attributed to phenolic monoterpenes such as thymol and carvacrol in TEO that can donate phenolic hydroxyl groups to capture free radicals [41]. The GSP-SA group showed obvious decolorization of both purple and blue-green colors because GSP contains abundant phenolic hydroxyl groups that can provide hydrogen atoms to neutralize free radicals and interrupt radical chain reactions [42]. Notably, the GSP-TEO-SA group completely lost the deep purple and deep blue-green colors and turned yellow-brown, indicating that the combined system had superior antioxidant activity to single-component films and suggesting a combined

antioxidant effect between GSP and TEO. The GSP-TEO-SA film exhibited the highest ABTS and DPPH scavenging rates, at 60.95 ± 1.90% and 33.82 ± 0.45%, respectively. The addition of TEO introduced phenolic compounds, which can neutralize free radicals by donating hydrogen atoms or electrons, thereby enhancing antioxidant capacity [43]. The antioxidant activity of the GSP-SA group was significantly higher than that of the SA group ($p < 0.05$), with scavenging rates increasing to 48.89 ± 3.06% for ABTS and 29.19 ± 0.30% for DPPH. This improvement is mainly attributed to the abundance of highly antioxidative phenolic hydroxyl groups in GSP, with studies indicating that its antioxidant activity surpasses that of anthocyanins [44].

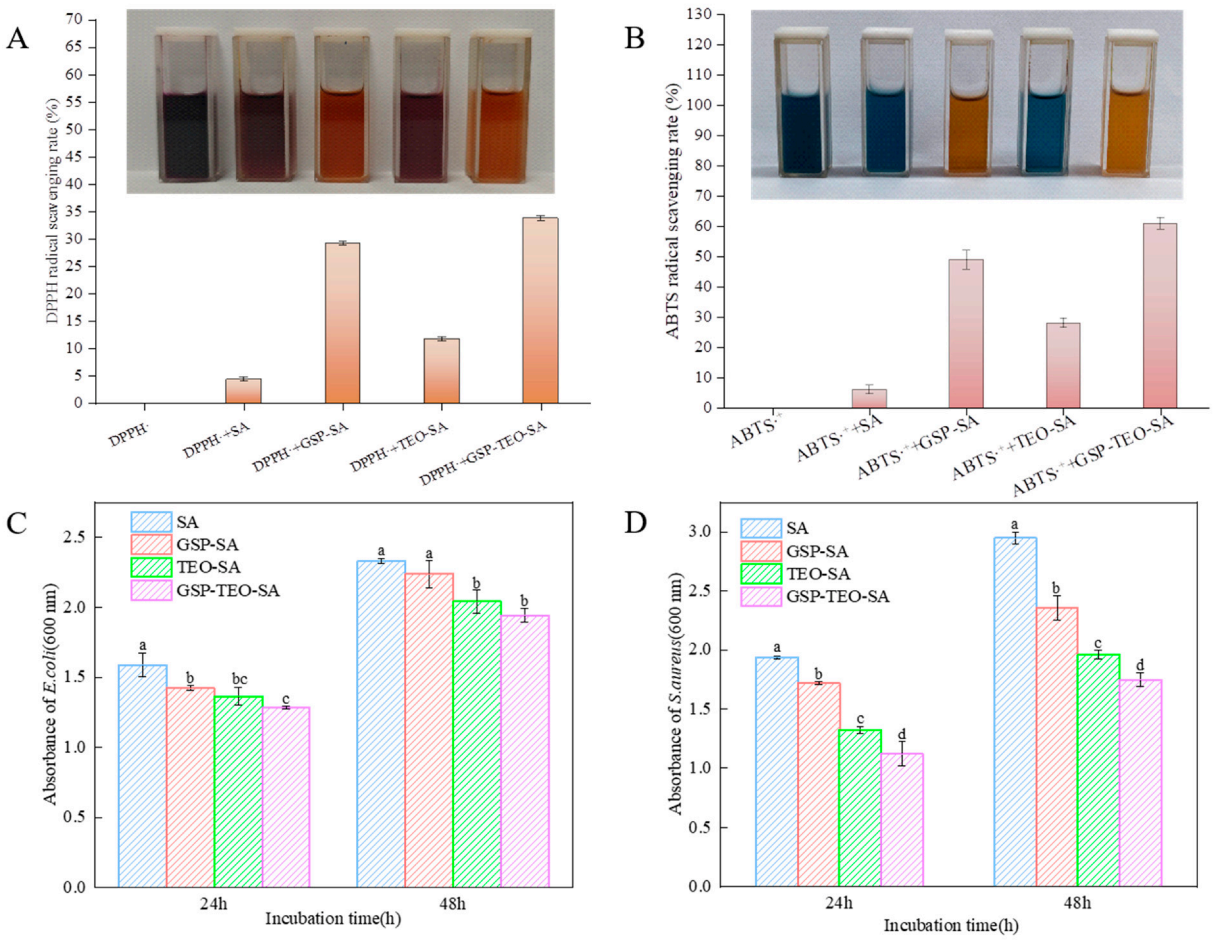


Figure 4. DPPH radical scavenging activity and visual color changes (**A**), ABTS radical scavenging activity and visual color changes (**B**), inhibitory effect of edible films against *E. coli* (**C**), and inhibitory effect of edible films against *S. aureus* (**D**). Note: Different letters indicate significant differences (a–d) ($p < 0.05$).

Among the four edible film groups, the TEO-SA and GSP-TEO-SA films exhibited better antibacterial effects against *E.coli* and *S.aureus*, which can be primarily attributed to the addition of TEO essential oil (Figure 4C,D) [11]. Essential oils possess broad-spectrum antimicrobial activity by disrupting bacterial cell walls and membranes [45]. Except for the SA membrane, there were significant differences in the antibacterial ability of the other three groups of membranes at the same culture time. GSP showed notable inhibitory effects against Gram-positive bacteria, leading to strong suppression of *S.aureus* by the films, with high activity maintained even after 24 h (Figure 4D). This mechanism may be related to the abundance of phenolic hydroxyl groups in GSP molecules, which can bind to bacterial enzymes, proteins, and DNA via hydrogen bonding, interfering with replication,

transcription, and protein synthesis, damaging membrane permeability, and ultimately resulting in bacterial death [46].

Figure 5A shows that the color of GSP is highly sensitive to environmental pH. The color shifts from a light yellowish-brown at pH 4 to a brownish-red at pH 7–8, and finally turns into a dark red with further increases in pH. This distinct visual change indicates that it is suitable for use as a pH-responsive material in edible films. Figure 5B shows that the color of GSP-SA and GSP-TEO-SA films gradually shifts from brownish-yellow to brownish-red and eventually to dark red as the pH increases from 4 to 12. This trend is consistent with the color transition observed in the GSP solution (Figure 5A). The results indicate that GSP can be used as a pH indicator in food packaging materials, and both films exhibit favorable pH-responsive properties across a broad pH range.

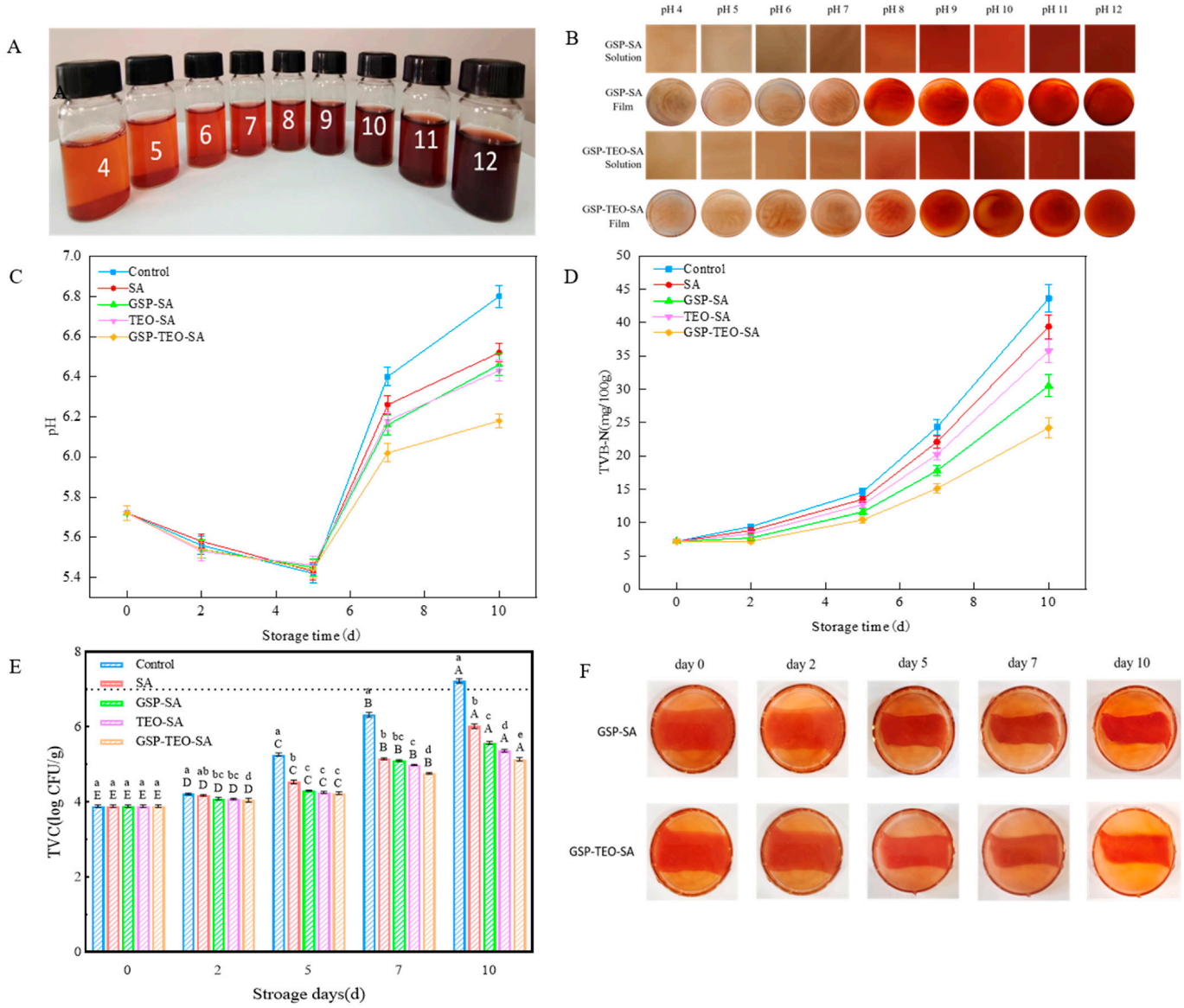


Figure 5. pH-responsive color changes in grape seed proanthocyanidins (**A**), color changes in GSP-SA and GSP-TEO-SA films under different pH conditions (**B**), pH changes in pork during storage (**C**), TVB-N changes in pork during storage (**D**), total viable count of pork loin wrapped with different edible films during storage (**E**), and color changes in edible films on pork loin during storage (**F**).

pH is an important indicator for evaluating meat spoilage. As shown in Figure 5C, the pH of all groups first decreased and then increased during storage. The initial decrease

was due to anaerobic glycolysis of muscle glycogen to lactic acid. After day 5, microbial proliferation and protein decomposition produced alkaline nitrogenous compounds, leading to a rapid increase in pH [47]. On day 10, the pH of the control group reached 6.79, exceeding the spoilage threshold of 6.7 [48], whereas all film-wrapped groups remained below the threshold. The GSP-TEO-SA film exhibited the best effect, with a pH of only 6.18 on day 10, demonstrating that GSP and TEO had a combined effect in delaying the pH increase. Note: Different lowercase letters (a–e) indicate significant differences among different groups on the same day, while different uppercase letters (A–E) indicate significant differences for the same group on different days.

TVB-N is a core indicator for evaluating meat freshness; higher values indicate more severe spoilage. During storage, microbial growth decomposes proteins into ammonia, amines, and other alkaline nitrogenous substances, increasing TVB-N. A value greater than 20 mg/100 g indicates that the meat has spoiled [49]. As shown in Figure 5D, TVB-N in all groups increased with storage time. The control group increased fastest and exceeded the spoilage threshold on day 7. The pure SA group followed, indicating the limited ability of the SA film to inhibit spoilage. The GSP-SA and TEO-SA groups showed slower increases, and the GSP-TEO-SA group was the most significant, reaching only 15.1 mg/100 g on day 7, which did not exceed the threshold [50]. This is because the phenolic structure of GSP can scavenge free radicals and has antibacterial activity, while thymol in TEO can disrupt the cell membranes of spoilage bacteria and inhibit their metabolism [51]. With increasing storage time, the TVB-N of all groups exceeded the threshold by day 10. In contrast, the GSP-TEO-SA film group maintained the lowest TVB-N level. The combined effect of GSP and TEO achieved optimal preservation, inhibiting protein decomposition and reducing the accumulation of spoilage metabolites.

Fresh pork tenderloin was used to evaluate the preservation effect of edible films, with a total bacterial count threshold of 7 lgCFU/g [52]. As shown in Figure 5E, the control group reached a total bacterial count of 7.22 ± 0.11 lgCFU/g on day 10, exceeding the threshold. In contrast, all film-coated groups remained below the threshold, with the GSP-TEO-SA group showing the lowest bacterial count of 5.14 ± 0.08 lgCFU/g, a reduction of 2.08 lgCFU/g compared with the control group, indicating that the film had significant antibacterial preservation effects. Similar observations have been reported in fish preservation studies [53].

The color changes in the edible films during pork tenderloin preservation are shown in Figure 5F. As storage time increased, the color of the GSP-TEO-SA film exhibited a trend of first lightening and then darkening, which aligned with the pattern of pH changes in pork tenderloin, where the pH first decreased and then increased within 120 h [54]. In contrast, the GSP-SA film without TEO showed smaller color variations and poorer synchronization with pH changes. These results indicate that TEO can effectively enhance the pH-responsive sensitivity and stability of GSP-based films, further demonstrating the potential of GSP-TEO-SA film as a visual freshness indicator for meat products.

4. Conclusions

In this study, pH-responsive edible films were prepared using sodium alginate (SA), grape seed proanthocyanidin (GSP), and thyme essential oil (TEO). Structural analysis indicated that GSP enhanced the film's compactness and thermal stability via hydrogen bonding, while TEO improved its flexibility and hydrophobicity. In terms of bioactivity, GSP imparted antioxidant properties to the film, whereas TEO contributed antibacterial effects. Their combined interaction endowed the GSP-TEO-SA film with optimal overall performance. Preservation tests on pork tenderloin demonstrated that the GSP-TEO-SA film significantly inhibited microbial growth ($p < 0.05$). The total viable count remained

consistently below 7 log CFU/g, while the TVB-N and pH values were also much lower than those of the control group. Furthermore, the color changes in the film aligned with pH variations, indicating its potential for freshness monitoring. The present work only qualitatively observed the pH-responsive color changes in the film, and quantitative characterization of color difference parameters was lacking. In future work, a colorimeter could be used for quantitative measurements to comprehensively evaluate its visual indication performance. Additionally, although the film exhibited intrinsic antioxidant activity, the antioxidant effect of the film in the pork system was not evaluated using lipid oxidation indicators (such as TBARS), which should be explored in future studies. In conclusion, the GSP-TEO-SA film integrates antibacterial, antioxidant, and pH-responsive functions, endowing it with potential for intelligent packaging and providing a reference for the development of future active food packaging systems.

Author Contributions: Conceptualization, J.S.; data curation, Y.C.; formal analysis, X.W.; funding acquisition, J.S.; investigation, G.Y. and P.L.; methodology, Z.Y., Y.L. (Yakun Li) and L.W.; project administration, J.S.; resources, P.L.; writing—original draft preparation, G.Y.; writing—review and editing, J.S.; visualization, Y.L. (Yulin Liu); validation, X.W. All authors have read and agreed to the published version of the manuscript.

Funding: This work was financially supported by the Henan Province International Science and Technology Cooperation Project (No. 262102520068), the Pingdingshan Science and Technology Innovation Outstanding Talents Program (No. 2017010(10.4)), Henan Key Scientific Research Projects (No. 25B550022), and the Innovative Training Program for College Students in Henan Province (No. 202611765027).

Institutional Review Board Statement: Not applicable.

Informed Consent Statement: Not applicable.

Data Availability Statement: Data will be made available upon request.

Conflicts of Interest: We hereby disclose our conflict of interest as outlined by the MDPI guidelines. Yakun Li and Peipei Li are currently employed by Henan Fengrui Food Co., Ltd. and were employed by Henan Fengrui Food Co., Ltd. while contributing to this manuscript. Our contributions to this work and manuscript were made independently without any requirement, guidance or input by our employer. We received no financial compensation from any source for the contributions we made to this scientific work and manuscript.

References

1. Pascall, M.A.; DeAngelo, K.; Richards, J.; Arensberg, M.B. Role and importance of functional food packaging in specialized products for vulnerable populations: Implications for innovation and policy development for sustainability. *Foods* **2022**, *11*, 3043. [CrossRef]
2. Han, J.W.; Ruiz-Garcia, L.; Qian, J.P.; Yang, X.T. Food packaging: A comprehensive review and future trends. *Compr. Rev. Food Sci. Food Saf.* **2018**, *17*, 860–877. [CrossRef]
3. Narayanan, M.; Loganathan, S.; Valapa, R.B.; Thomas, S.; Varghese, T.O. UV protective poly(lactic acid)/rosin films for sustainable packaging. *Int. J. Biol. Macromol.* **2017**, *99*, 37–45. [CrossRef]
4. Chiu, I.; Ye, H.; Aayush, K.; Yang, T. Intelligent food packaging for smart sensing of food safety. *Adv. Food Nutr. Res.* **2024**, *111*, 215–259. [CrossRef]
5. Ghaani, M.; Cozzolino, C.A.; Castelli, G.; Farris, S. An overview of the intelligent packaging technologies in the food sector. *Trends Food Sci. Technol.* **2016**, *51*, 1–11. [CrossRef]
6. Kanatt, S.R. Development of active/intelligent food packaging film containing *Amaranthus* leaf extract for shelf life extension of chicken/fish during chilled storage. *Food Packag. Shelf Life* **2020**, *24*, 100506. [CrossRef]
7. Bierhalz, A.C.K.; da Silva, M.A.; Braga, M.E.M.; Sousa, H.J.C.; Kieckbusch, T.G. Effect of calcium and/or barium crosslinking on the physical and antimicrobial properties of natamycin-loaded alginate films. *LWT-Food Sci. Technol.* **2014**, *57*, 494–501. [CrossRef]
8. Almasi, H.; Azizi, S.; Amjadi, S. Development and characterization of pectin films activated by nanoemulsion and Pickering emulsion stabilized marjoram (*Origanum majorana* L.) essential oil. *Food Hydrocoll.* **2020**, *99*, 105338. [CrossRef]

9. Sánchez-Ordóñez, M.; Orts, I.; Martillanes, S.; Ramírez-Bernabé, M.D.R.; Delgado-Adámez, J. Chitosan-based active films enriched with thyme essential oil for extending the shelf life of refrigerated chicken meat. *Foods* **2026**, *15*, 3347. [CrossRef]
10. Guzmán-Pincheira, C.; Moeini, A.; Oliveira, P.E.; Abril, D.; Paredes-Padilla, Y.A.; Benavides-Valenzuela, S. Development of alginate-chitosan bioactive films containing essential oils for use in food packaging. *Foods* **2025**, *14*, 256. [CrossRef]
11. Liu, Z.; Lin, D.; Shen, R.; Zhang, R.; Liu, L.; Yang, X. Konjac glucomannan-based edible films loaded with thyme essential oil: Physical properties and antioxidant-antibacterial activities. *Food Packag. Shelf Life* **2021**, *29*, 100700. [CrossRef]
12. Andretta, R.; Luchese, C.L.; Tessaro, I.C.; Spada, J.C. Development and characterization of pH-indicator films based on cassava starch and blueberry residue by thermocompression. *Food Hydrocoll.* **2019**, *93*, 317–324. [CrossRef]
13. Prietto, L.; Mirapalhete, T.C.; Pinto, V.Z.; Hoffmann, J.F.; Vanier, N.L.; Lim, L.T.; Guerra Dias, A.R.; da Rosa Zavareze, E. PH-sensitive films containing anthocyanins extracted from black bean seed coat and red cabbage. *LWT-Food Sci. Technol.* **2017**, *80*, 492–500. [CrossRef]
14. Vrabič-Brodnjak, U.; Ružič, T. Bio-based alginate films incorporating bacterial nanocellulose and grape seed extract for enhanced food packaging. *Polymers* **2025**, *17*, 2564. [CrossRef]
15. Wu, H.; Li, T.; Peng, L.; Wang, J.; Lei, Y.; Li, S.; Li, Q.; Yuan, X.; Zhou, M.; Zhang, Z. Development and characterization of antioxidant composite films based on starch and gelatin incorporating resveratrol fabricated by extrusion compression moulding. *Food Hydrocoll.* **2023**, *139*, 108509. [CrossRef]
16. Tan, L.F.; Elaine, E.; Pui, L.P.; Nyam, K.L.; Yusof, Y.A. Development of chitosan edible film incorporated with *Chrysanthemum morifolium* essential oil. *Acta Sci. Pol. Technol. Aliment.* **2021**, *20*, 55–66. [CrossRef]
17. Zhao, R.; Guan, W.; Zhou, X.; Lao, M.; Cai, L. The physiochemical and preservation properties of anthocyanidin/chitosan nanocomposite-based edible films containing cinnamon-perilla essential oil pickering nanoemulsions. *LWT-Food Sci. Technol.* **2022**, *153*, 112506. [CrossRef]
18. Sun, R.; Zhu, J.; Wu, H.; Wang, S.; Li, W.; Sun, Q. Modulating layer-by-layer assembled sodium alginate-chitosan film properties through incorporation of cellulose nanocrystals with different surface charge densities. *Int. J. Biol. Macromol.* **2021**, *180*, 510–522. [CrossRef]
19. Sun, J.; Wang, L.; Chen, H.; Yin, G. Enhancing biodegradable packaging: The role of tea polyphenols in soybean oil body emulsion films. *Coatings* **2025**, *15*, 162. [CrossRef]
20. Yuan, L.; Feng, W.; Zhang, Z.; Peng, Y.; Xiao, Y.; Chen, J. Effect of potato starch-based antibacterial composite films with thyme oil microemulsion or microcapsule on shelf life of chilled meat. *LWT-Food Sci. Technol.* **2021**, *139*, 110462. [CrossRef]
21. Zhang, W.; Jiang, W. Antioxidant and antibacterial chitosan film with tea polyphenols-mediated green synthesis silver nanoparticle via a novel one-pot method. *Int. J. Biol. Macromol.* **2020**, *155*, 1252–1261. [CrossRef]
22. Wu, Z.; Li, Y.; Tang, J.; Lin, D.; Qin, W.; Loy, D.A.; Zhang, Q.; Chen, H.; Li, S. Ultrasound-assisted preparation of chitosan/nano-silica aerogel/tea polyphenol biodegradable films: Physical and functional properties. *Ultrason. Sonochem.* **2022**, *87*, 106052. [CrossRef]
23. Kadam, D.; Momin, B.; Palamthodi, S.; Lele, S.S. Physicochemical and functional properties of chitosan-based nano-composite films incorporated with biogenic silver nanoparticles. *Carbohydr. Polym.* **2019**, *211*, 124–132. [CrossRef]
24. Guzman-Puyol, S.; Benítez, J.J.; Heredia-Guerrero, J.A. Transparency of polymeric food packaging materials. *Food Res. Int.* **2022**, *161*, 111792. [CrossRef]
25. Wang, Q.; Chen, W.; Ma, C.; Chen, S.; Liu, X.; Liu, F. Enzymatic synthesis of sodium caseinate-EGCG-carboxymethyl chitosan ternary film: Structure, physical properties, antioxidant and antibacterial properties. *Int. J. Biol. Macromol.* **2022**, *222*, 509–520. [CrossRef]
26. Liu, J.; Wang, Y.; Lv, J.; Wu, Y.; Guo, Y.; Sun, C.; Li, X. Biodegradable composite films based on egg white protein and tea polyphenol: Physicochemical, structural and antibacterial properties. *Food Packag. Shelf Life* **2023**, *38*, 101098. [CrossRef]
27. Ghasempour, Z.; Khodaeivandi, S.; Ahangari, H.; Hamishehkar, H.; Amjadi, S.; Moghaddas, K.E.; Ehsani, A. Characterization and optimization of persian gum/whey protein bionanocomposite films containing betanin nanoliposomes for food packaging utilization. *J. Polym. Environ.* **2022**, *30*, 2800–2811. [CrossRef]
28. Guo, H.; Yue, Z.; Shao, C.; Shao, C.; Han, Y.; Li, S.; Miao, Z.; Gao, S.; Li, J.; Li, Y.; et al. Intelligent carboxymethyl cellulose composite films containing *Garcinia mangostana* shell anthocyanin with improved antioxidant and antibacterial properties. *Int. J. Biol. Macromol.* **2024**, *263*, 130362. [CrossRef]
29. Zhu, J.Y.; Tang, C.H.; Yin, S.W.; Yang, X.Q. Development and characterization of novel antimicrobial bilayer films based on polylactic acid (PLA)/Pickering emulsions. *Carbohydr. Polym.* **2018**, *181*, 727–735. [CrossRef]
30. Yao, F.; Zheng, Y.; Gao, Y.; Du, Y.; Chen, F. Electrospinning of peanut protein isolate/poly-L-lactic acid nanofibers containing tetracycline hydrochloride for wound healing. *Ind. Crops Prod.* **2023**, *194*, 116262. [CrossRef]
31. Teymoorian, M.; Moghimi, R.; Hosseinzadeh, R.; Zandi, F.; Lakouraj, M.M. Fabrication the emulsion-based edible film containing *Dracocephalum kotschyi* Boiss essential oil using chitosan-gelatin composite for grape preservation. *Carbohydr. Polym. Technol. Appl.* **2024**, *7*, 100444. [CrossRef]

32. Li, S.; Lu, W.; Tang, Q.; Xiao, Q.; Kang, Y.; Hu, L.; Huang, Y.; Peng, C.; Yang, H. Preparation of super hydrophilic sodium alginate/chitosan-Ag composite membranes with antibacterial activity for effective oil-water emulsion separation. *Chem. Eng. Sci.* **2024**, *285*, 119547. [CrossRef]
33. Zhao, L.; Liu, Y.; Zhao, L.; Wang, Y. Anthocyanin-based pH-sensitive smart packaging films for monitoring food freshness. *J. Agric. Food Res.* **2022**, *9*, 100340. [CrossRef]
34. Gouda, M.; Khalaf, M.M.; Alghamdi, A.; Taleb, M.F.A.; Zidan, N.S.; El-Lateef, H.M.A. Formulation and biological evaluation of sodium alginate-based films blended with watercress oil: A promising solution for combating foodborne pathogens and potential food packaging applications. *Food Chem.* **2025**, *473*, 143089. [CrossRef]
35. Alizadeh-Sani, M.; Tavassoli, M.; McClements, D.J.; Hamishehkar, H. Multifunctional halochromic packaging materials: Saffron petal anthocyanin loaded-chitosan nanofiber/methyl cellulose matrices. *Food Hydrocoll.* **2021**, *111*, 106237. [CrossRef]
36. Nguyen, T.T.; Pham, B.T.T.; Le, H.N.; Bach, L.G.; Thuc, C.N.H. Comparative characterization and release study of edible films of chitosan and natural extracts. *Food Packag. Shelf Life* **2022**, *32*, 100830. [CrossRef]
37. Criado, P.; Fraschini, C.; Jamshidian, M.; Salmieri, S.; Desjardins, N.; Sahraoui, A.; Lacroix, M. Effect of cellulose nanocrystals on thyme essential oil release from alginate beads: Study of antimicrobial activity against *Listeria innocua* and ground meat shelf life in combination with gamma irradiation. *Cellulose* **2019**, *26*, 5247–5265. [CrossRef]
38. Song, J.; Zhang, S.; Du, L.; Gao, C.; Xie, L.; Shi, Y.; Su, L.; Ma, Y.; Ren, S. Synthesis, characterization and application of oligomeric proanthocyanidin-rich dual network hydrogels. *Sci. Rep.* **2023**, *13*, 17754. [CrossRef]
39. Xu, Y.; Willis, S.; Jordan, K.; Sismour, E. Chitosan nanocomposite films incorporating cellulose nanocrystals and grape pomace extracts. *Packag. Technol. Sci.* **2018**, *31*, 631–638. [CrossRef]
40. Liu, D.; Dang, S.; Zhang, L.; Munsop, K.; Li, X. Corn starch/polyvinyl alcohol based films incorporated with curcumin-loaded Pickering emulsion for application in intelligent packaging. *Int. J. Biol. Macromol.* **2021**, *188*, 974–982. [CrossRef]
41. Dobreva, K.; Dimov, M.; Valev, T.; Iliev, I.; Damyanova, S.; Oprea, O.B.; Stoyanova, A. Chemical composition and antioxidant activities of three bulgarian garden thyme essential oils. *Appl. Sci.* **2024**, *14*, 10261. [CrossRef]
42. Yang, D.S.; Zhang, L.P.; Gao, S.; Luo, Y.L.; Luo, R.M.; Hou, Y.R. Effects of grape seed proanthocyanidin on the conformation and functional properties of lamb myofibrillar protein under hydroxyl radical-induced oxidative stress. *LWT-Food Sci. Technol.* **2025**, *222*, 117625. [CrossRef]
43. Sayadi, M.; Abedi, E.; Oliyaei, N. Effect of persian gum-gelatin based-pickering emulsion film loaded with thyme essential oil on the storage quality of barred mackerel (*Scomberomorus commerrson*)fillet. *LWT-Food Sci. Technol.* **2025**, *215*, 117241. [CrossRef]
44. Huang, W.; Lin, S.; Wu, X.; Wu, H.; Chen, S.; Cao, H.; Xiao, J. Unveiling grape seed extract phytochemical composition, antioxidant, and immunostimulant action mechanisms in Caenorhabditis elegans and Drosophila melanogaster. *Food Biosci.* **2025**, *71*, 107184. [CrossRef]
45. Falleh, H. Demystifying the power of essential oils: A review of their antibacterial properties and potential as natural food preservatives. *Excli J.* **2025**, *24*, 828–850. [CrossRef]
46. Ashrafi, A.; Jokar, M.; Nafchi, A.M. Preparation and characterization of biocomposite film based on chitosan and kombucha tea as active food packaging. *Int. J. Biol. Macromol.* **2018**, *108*, 444–454. [CrossRef]
47. Zheng, K.W.; Zhang, J.B.; Yang, F.; Wang, W.; Li, W.; Qin, C.Q. Properties and biological activity of chitosan-coix seed starch films incorporated with nano zinc oxide and Artemisia annua essential oil for pork preservation. *LWT-Food Sci. Technol.* **2022**, *163*, 113665. [CrossRef]
48. Cai, J.; Gao, X.Y.; Wang, J.F.; Lv, H.J. PH-responsive active packaging based on chitosan films embedded with grape skin anthocyanins/thymol nanoparticles: Preparation, characterization, and pork preservation application. *Food Res. Int.* **2026**, *236*, 119252. [CrossRef]
49. Tan, S.; Chen, W.Y.; Wang, L.K.; Xu, L.L.; Wang, J.Y.; Han, G.Q.; Zhang, W.L. Preparation of starch/sodium carboxymethylcellulose films incorporated with Carmine radish anthocyanin, tea polyphenol, and curcumin for pork and shrimp preservation. *LWT-Food Sci. Technol.* **2026**, *254*, 119733. [CrossRef]
50. Krasteva, D.; Ivanov, Y.; Chengolova, Z.; Godjevargova, T. Antimicrobial potential, antioxidant activity, and phenolic content of grape seed extracts from four grape varieties. *Microorganisms* **2023**, *11*, 395. [CrossRef]
51. Kou, X.; Gong, J.F.; Huang, X.; Zhang, Y.C.; Meng, Q.R.; Ke, Q.F.; Yang, X.X. Encapsulation of thyme essential oil: A review of mechanistic insights and emerging applications. *Food Chem.* **2026**, *526*, 150758. [CrossRef]
52. Xiong, Y.; Li, S.; Warner, R.D.; Fang, Z. Effect of oregano essential oil and resveratrol nanoemulsion loaded pectin edible coating on the preservation of pork loin in modified atmosphere packaging. *Food Control* **2020**, *114*, 107226. [CrossRef]

53. Shao, Z.; Lan, W.; Xie, J. A konjac glucomannan/gelatin film integrated with rosemary essential oil and ginger essential oil-loaded bacterial cellulose: Preparation, characterization, and application in sea bass (*Lateolabrax maculatus*) packaging. *Food Chem.* **2025**, *478*, 143604. [CrossRef]
54. Liu, T.; Liu, L.; Gong, X.; Chi, F.; Ma, Z. Fabrication and comparison of active films from chitosan incorporating different spice extracts for shelf life extension of refrigerated pork. *LWT-Food Sci. Technol.* **2021**, *135*, 110181. [CrossRef]

Disclaimer/Publisher's Note: The statements, opinions and data contained in all publications are solely those of the individual author(s) and contributor(s) and not of MDPI and/or the editor(s). MDPI and/or the editor(s) disclaim responsibility for any injury to people or property resulting from any ideas, methods, instructions or products referred to in the content.